



A Semi-Analytical Study on Multiscale Porous Biocatalytic Electrodes in the Enzyme Reaction Process

V. Vijayalakshmi¹ , V. Ananthaswamy^{*2}  and J. Anantha Jothi³ 

Research Centre and PG Department of Mathematics, The Madura College (affiliated to Madurai Kamaraj University), Madurai, Tamil Nadu, India

*Corresponding author: ananthu9777@gmail.com

Received: July 14, 2024

Accepted: October 26, 2024

Abstract. A multiscale porous biocatalytic electrode's oxidation of glucose is explained theoretically. The model that describes diffusion and response within a hydrogel film is composed by two non-linear differential equations. Approximate analytical findings of the glucose concentrations, current, and the oxidised mediator have been obtained via the new homotopy perturbation technique. Furthermore, an analytical calculation is performed to determine the ideal electrode thickness for the film by employing Ananthaswamy-Sivasankari Method (ASM). It also investigates how parameters affect current. Our approximate analytical expressions are validated by the numerical simulation (MATLAB).

Keywords. Bioelectrodes, Glucose oxidase, New Homotopy Perturbation Method (NHPM), Ananthaswamy-Sivasankari Method (ASM), Non-linear boundary value problem, Numerical Simulation

Mathematics Subject Classification (2020). 34B15, 34E05, 34E10, 34E15

Copyright © 2024 V. Vijayalakshmi, V. Ananthaswamy and J. Anantha Jothi. *This is an open access article distributed under the Creative Commons Attribution License, which permits unrestricted use, distribution, and reproduction in any medium, provided the original work is properly cited.*

1. Introduction

Porous electrodes are currently of great interest from both a theoretical and practical point of view. The design of miniature electro devices such as biobatteries, enzymatic reactors, biofuel cells, and biosensors depends on such enzymatic electrodes (Cosnier *et al.* [8], Do *et al.* [9], and Leech *et al.* [17]). Using a direct electron transfer, Do *et al.* [9] created one-dimensional complete along with reduced porous electrode systems to replicate and examine the behaviour of an enzyme porous electrode. According to Barcia *et al.* [4], electrochemical

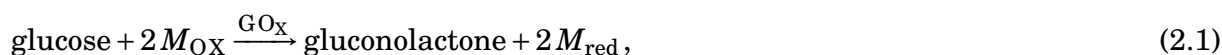
impedance spectroscopy serves as an extremely beneficial method for figuring out the properties of porous electrodes. Galceran *et al.* [10] used an iterative approach for the finite element technique to calculate the time independent currents on an inlaid microdisc electrode of an enzyme-catalyzed reaction that is mediated by redox.

An electro-deposition theory for simulating cyclic voltammetry and chronoamperometry on porous electrodes constructed round spherical templates was provided to Barnes *et al.* [5]. By approximating the decoupling for bulk diffusion for the surface in electrode along with diffusion inside a porous electrode, a theoretic approach for extracting rate constants for heterogeneous in the systems and irreversible as well as quasireversible had been presented. Nam and Bonnecaze [21] used known flow field results over an infinite porous rotating disk to build analytical models on the advection-dominated as well as diffusion-dominated regimes on the porous rotating disc electrode. In the enzyme-based biofuel cells (EBFC), supported glucose oxidase and mediator immobilise, Chan *et al.* [7] develop a dynamic model that simulates the anode's discharge performance. Ke *et al.* [16] present a three-dimensional representation for a serpentine flow field across a porous carbon electrode within a flow battery. Considering the model system of glucose oxidation catalysed by glucose oxidase, Wen *et al.* [25] reported a quantitative investigation related to reaction as well as transport within porous biocatalytic electrodes on multiscale. Bartlett and Pratt *et al.* [6] give a thorough analysis about the diffusion as well as reaction inside a uniform film comprising immobilised enzyme and also mediator over an electrode surface.

This work aims to get approximate analytical formulas to calculate the non-dimensional concentration of both the redox mediator and substrate by utilising NHPM. This approach requires a single iteration compared to other numerical and approximate analytical expressions. A comparison and graphical display are then performed between the approximate analytical expressions and the numerical simulation. Graphical representations are employed to illustrate the effect for a several parameters, including the relative amount of depletion, the saturation parameter, and the enzymatic reaction. Additionally, current is calculated by employing NHPM. ASM is utilized to solve the non-dimensional concentration inside the porous electrode.

2. Mathematical Structure of the Problem

The chemical reaction taking place inside the motorbike porous electrode is able to explained by the following (Wen *et al.* [25]):



The substrate (glucose) S , is oxidised with the help of the enzyme glucose oxidase (GO_x), as shown in equation (2.1). Furthermore, equation (2.2) represents the mediator's reoxidation at the electrode surface, which generates the current. The oxidised mediator as well as the substrate within the hydrogel sheet in ping-pong bi-bi enzyme kinetics can be represented using the following one-dimensional mass balance equations (Wen *et al.* [25]),

$$D_M \frac{d^2 M_{OX}(x)}{dx^2} - \frac{k_{cat} E \cdot S(x) M_{OX}(x)}{K_S M_{OX}(x) + K_M S(x) + S(x) M_{OX}(x)} = 0, \quad (2.3)$$

$$D_S \frac{d^2 S(x)}{dx^2} - \frac{k_{cat} E \cdot S(x) M_{ox}(x)}{2(K_S M_{ox}(x) + K_M S(x) + S(x) M_{ox}(x))} = 0, \tag{2.4}$$

where M_{ox} denotes the oxidized mediator S represents the substrate, and E indicates the enzyme concentrations (mol cm⁻³), respectively. Here, x denotes the location within the hydrogel film's thickness. Equations (2.3) and (2.4) holds the boundary conditions as shown below:

$$x = 0, M_{ox}(x) = \frac{M_0}{(1 + e^{-\epsilon})}, \frac{ds(x)}{dx} = 0, \tag{2.5}$$

$$x = l, \frac{dM_o(x)}{dx} = 0, S(x) = S_0. \tag{2.6}$$

M_o is the mediator's reference concentration and S_0 is the substrate's reference concentration (mol cm⁻³), respectively. The non-dimensional potential is provided by $\epsilon = \frac{(E - E_0)nF}{RT}$.

The current density i on the surface of electrode is calculated as

$$i(S) = 2Fj(S) = 2FD_S \left. \frac{ds}{dx} \right|_{x=1}. \tag{2.7}$$

To simplify equations (2.3) and (2.4) into a non-dimensional form, the following non-dimensional variable will be introduced

$$M = \frac{M_{red}}{M_o}, S = \frac{S}{S_o}, X = \frac{x}{l}, \kappa = l \sqrt{\frac{k_{cat} E}{D_M M_o}}, \mu = \frac{K_M}{M_o}, \sigma = \frac{K_S}{S_o}, \eta = \frac{D_S S_o}{D_M M_o}. \tag{2.8}$$

The oxidised mediator and substrate concentration's in non-dimensional are denoted by M and S . X represents the non-dimensional distance from the film interface. The remaining parameters are enzymatic reaction κ , saturation parameters μ , σ and η relative amount of the depletion. Utilizing equation (2.8), we attain the subsequent non-dimensional equation for the planar film model,

$$\frac{d^2 M}{dX^2} - \frac{\kappa^2 S(x) M(x)}{\sigma M(x) + \mu S(x) + S(x) M(x)} = 0, \tag{2.9}$$

$$\frac{d^2 S}{dX^2} - \frac{\kappa^2 S(x) M(x)}{\eta(\sigma M(x) + \mu S(x) + S(x) M(x))} = 0. \tag{2.10}$$

The respective boundary conditions for equations (2.9) and (2.10) are

$$X = 0, M = \frac{1}{(1 + e^{-\epsilon})} = M_\epsilon, \frac{dS}{dX} = 0, \tag{2.11}$$

$$X = 1, \frac{dM}{dX} = 0, S = 1. \tag{2.12}$$

The non-dimensional current ψ is given as follows

$$\psi = \left. \frac{dS}{dX} \right|_{X=1}. \tag{2.13}$$

2.1 Porous Electrode Model

Based on the concept previously mentioned, the autonomous mobile species within the porous electrode represents the substrate. The substrate concentration within the porous electrode can be found using the diffusion as well as convection equation, as mentioned by Wen *et al.* [25],

$$\epsilon_g D_S S''(y) + v \frac{dS}{dy} = a j(S). \tag{2.14}$$

The boundary conditions are:

$$\text{at } y = 0, \quad \frac{dS}{dy} = 0, \quad (2.15)$$

$$\text{at } y = L, \quad S = S_0, \quad (2.16)$$

where ε_g denotes porosity of the film-loaded toray carbon paper, D_S indicates the diffusion coefficient for substrate, v represents the velocity of fluid element, a denotes the surface area per unit volume of the toray carbon paper, j denotes the flux and y indicates the position within the porous electrode. Also, L represent the thickness of the toray carbon paper and S_0 represents the reference concentration for mediator.

The following non-dimensional variables are introduced.

$$s = \frac{S}{S_0}, \quad Y = \frac{y}{l}, \quad Pe = \frac{vL}{D_S}, \quad \delta = \frac{aL^2}{l}. \quad (2.17)$$

Here s is the non-dimensional substrate concentration, Y denotes the position within the porous electrode, Pe represent the pecllet number, δ indicates the dimensionless area of the toray carbon paper.

By utilizing the above mentioned non-dimensional variables, equation (2.14) can be diminished as follows

$$\frac{d^2s(y)}{dY^2} + \frac{Pe}{\varepsilon_g} \cdot \frac{ds(y)}{dY} = \frac{\delta\psi}{\varepsilon_g}. \quad (2.18)$$

The associated non-dimensional boundary conditions are provided by

$$\text{at } Y = 0, \quad \frac{ds}{dY} = 0, \quad (2.19)$$

$$\text{at } Y = 1, \quad s = 1. \quad (2.20)$$

Y is the position within the porous electrode.

3. Approximate Analytical Expressions

3.1 Approximate Analytical Expression for equations (2.9)-(2.12) by Utilizing New Homotopy Perturbation Technique

Both linear as well as non-linear differential equations, which may model a broad variety of behaviours, have a major influence on numerous scientific and technological domains. There are several non-linear differential equations for which there are insufficient analytical solutions. The variational iterative technique by Wazwaz [24], homotopy perturbation approach by Meena and Rajendran [18], new homotopy perturbation technique by Mehala and Rajendran[19] and homotopy analysis technique by Rasi *et al.* [22], The adomian decomposition technique by Adomian [1] which are the some approximate analytical methods that are used for solving differential equations in non-linear approximately.

He proposed the *homotopy perturbation method* (HPM) to create analytical approximations ([11–15]). The most effective and practical way to get an approximate analytical solution for differential equations, both linear and non-linear, is through the use of HPM. A variety of boundary and initial value problems have been shown to respond well to the homotopy perturbation strategy by Mousa and Ragab [20]. The perturbation approach is predicated on the small-parameter assumption. The approximate analytical expressions attained by

perturbation technique can be appropriate over small amounts of minor parameters since the significant numbers of non-linear problems. Generally, perturbation solutions work just as well when the parameters of the scientific system are small. Since there is no standard for the presence of minor parameters, the approximation cannot be completely relied upon. Consequently, it is essential to confirm the approximation's accuracy both analytically and experimentally. HPM has recently been proposed as an alternative for these issues. He [13] then applies a novel method based on homotopy perturbation technique to the zeroth iteration of solving non-linear differential equations.

The semi-analytical expressions for the equations (2.9)-(2.10) in non-dimensional form by utilizing new homotopy perturbation technique (Ananthaswamy *et al.* [2, 3]) is given by:

$$M(x) = M_\varepsilon \frac{\cosh \sqrt{\gamma}(X-1)}{\cosh \sqrt{\gamma}}, \quad (3.1)$$

$$S(x) = \frac{\cosh \sqrt{\lambda}X}{\cosh \sqrt{\lambda}}, \quad (3.2)$$

where

$$\gamma = \frac{\kappa^2}{\sigma + \mu + 1}, \quad (3.3)$$

$$\lambda = \frac{\kappa^2}{\eta(\sigma + \mu + 1)}. \quad (3.4)$$

The current ψ is given by

$$\psi = \lambda \frac{\sinh(\lambda)}{\cosh(\lambda)}. \quad (3.5)$$

3.2 Approximate Analytical Expression for Equation (2.19) by Utilizing Ananthaswamy-Sivasankari Method (ASM)

A recently developed method for resolving second-order non-linear ordinary differential equations is known as the Ananthaswamy-Sivasankari Method (ASM) [23]. It can also be utilized to resolve non-linear and linear differential equations. This method can also be readily extended to handle a number of other non-linear issues in the physical, biological, and chemical sciences. The new approach that has been provided, though, can be used for boundary value problems.

The approximate analytical expression for equation (2.18) by utilizing Ananthaswamy-Sivasankari Method (ASM) as follows:

$$s(y) = \frac{\cosh(aY)}{\cosh(a)}, \quad (3.6)$$

where

$$a = -1.4741. \quad (3.7)$$

4. Numerical Simulation

For the differential equations that are non-linear, numerical simulation can verify the efficacy of our approximate analytical expression. MATLAB functions `pdex4` are employed for equations (2.9)-(2.12). The semi-analytical results and the numerical simulation show good agreement, as shown in Figures 1-2.

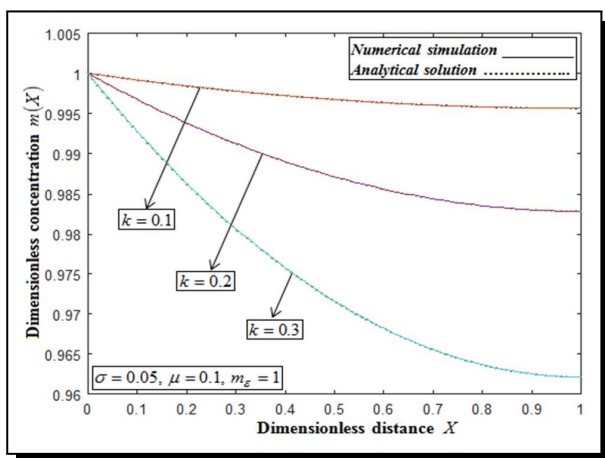
Table 1. Comparing the numerical simulation with our approximate analytical results (NHPM) eqn. (3.1) by setting the values of saturation parameters and ratio of enzymatic reaction

| X | k = 0.2 | | | k = 0.6 | | | k = 0.01 | | |
|--------------------------|-----------|------------|---------|-----------|------------|---------|-----------|------------|---------|
| | Numerical | NHPM (3.1) | Error % | Numerical | NHPM (3.1) | Error % | Numerical | NHPM (3.1) | Error % |
| 0 | 1 | 1 | 0.0000 | 1 | 1 | 0.0000 | 0.9826 | 0.9826 | 0.0000 |
| 0.2 | 0.9937 | 0.9938 | 0.0001 | 0.9445 | 0.9444 | 0.0001 | 0.9833 | 0.9834 | 0.0001 |
| 0.4 | 0.9889 | 0.9989 | 0.0000 | 0.9014 | 0.9012 | 0.0002 | 0.9854 | 0.9854 | 0.0000 |
| 0.6 | 0.9854 | 0.9855 | 0.0001 | 0.8706 | 0.8704 | 0.0002 | 0.9889 | 0.9888 | 0.0001 |
| 0.8 | 0.09833 | 0.9834 | 0.0001 | 0.8521 | 0.8519 | 0.0002 | 0.9937 | 0.9937 | 0.0000 |
| 1 | 0.9826 | 0.9827 | 0.0001 | 0.8460 | 0.8457 | 0.0003 | 1 | 1 | 0.0000 |
| Absolute Average Error % | | | 0.0001 | | | 0.0001 | | | 0.0001 |

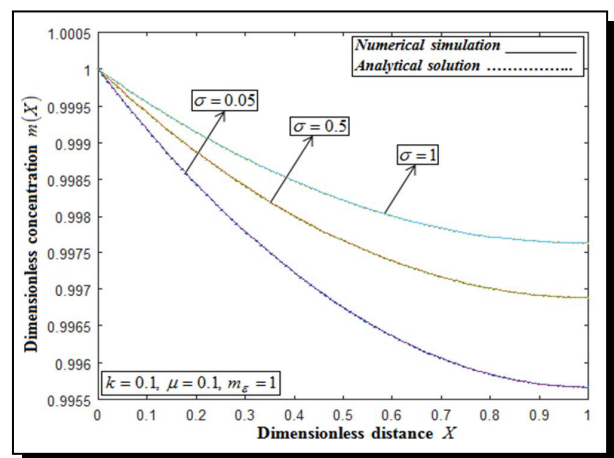
5. Results and Discussion

The semi-analytical findings for the concentrations of the substrate as well as the product are attained. In Figures 1-2 display that the comparison between the numerical simulation and the attained semi-analytical expressions. The numerical simulation of experimental data for all parameters agrees exactly with the approximate analytical expressions. From Table 1 we noted that the error percentage is < 0.0001% by comparing the numerical simulation and our approximate analytical results (NHPM).

Non-dimensional concentration of oxidised mediator. Figure 1 displays that the non-dimensional concentration of oxidised mediator M versus the non-dimensional distance X . The value of ratio of enzymatic reaction k get increases than the non-dimensional concentration falls, as shown in Figure 1(a). Figures 1(b) and 1(c) illustrates that the values of saturation parameter σ and μ get rises so does the non-dimensional concentration.

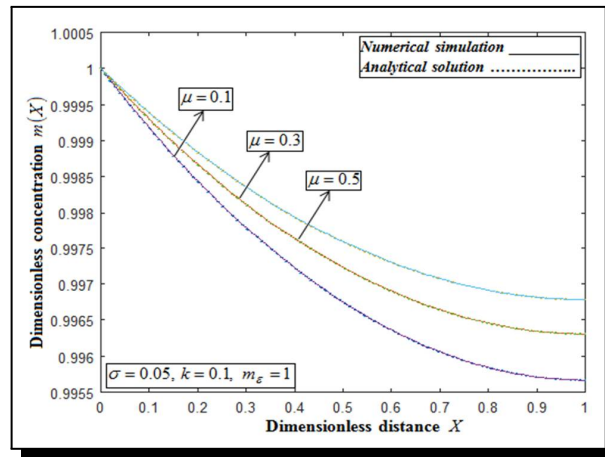


(a) Impact of ratio of enzymatic reaction k in non-dimensional concentration of oxidised mediator M



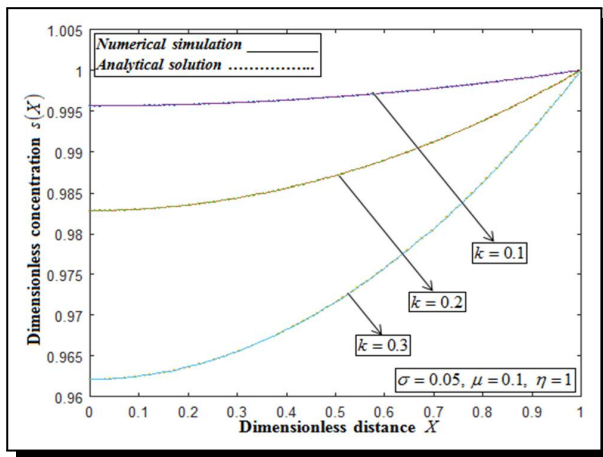
(b) Variation of saturation parameter σ in non-dimensional concentration of oxidised mediator M

(Figure continued)

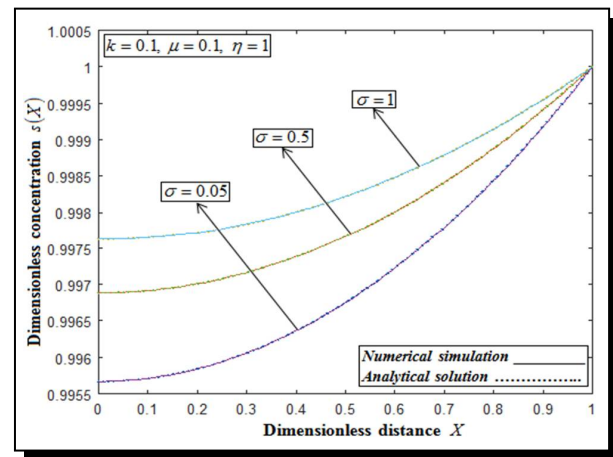


(c) Influence of saturation parameter μ in non-dimensional concentration of oxidised mediator M

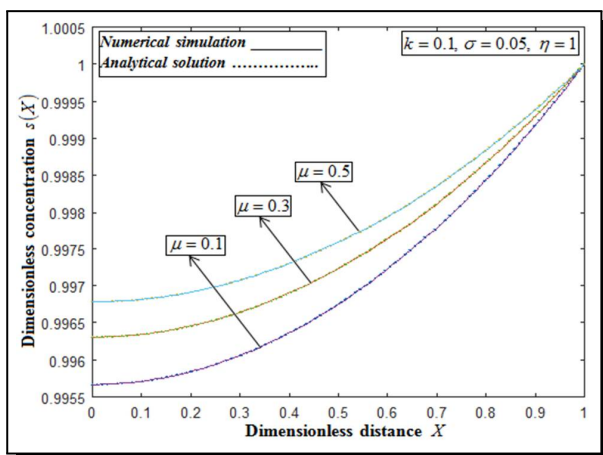
Figure 1



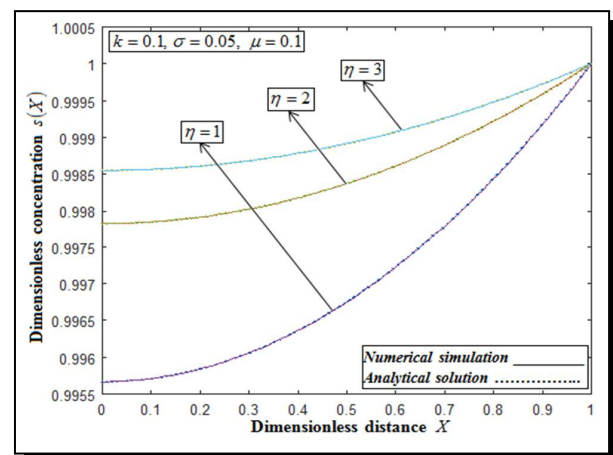
(a) Effect of ratio of enzymatic reaction k in non-dimensional concentration of substrate S



(b) Impact of saturation parameter σ in non-dimensional concentration of substrate S

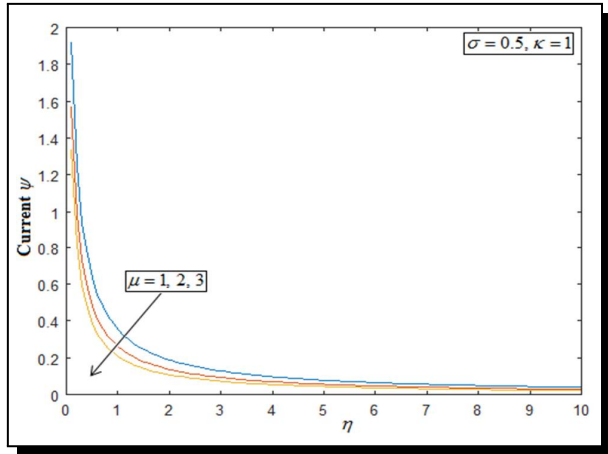


(c) Variation of saturation parameter μ in non-dimensional concentration of substrate S

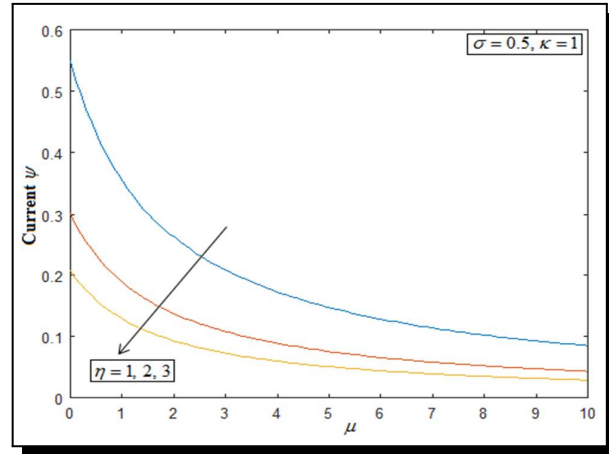


(d) Influence of relative amount of the depletion η in non-dimensional concentration of substrate S

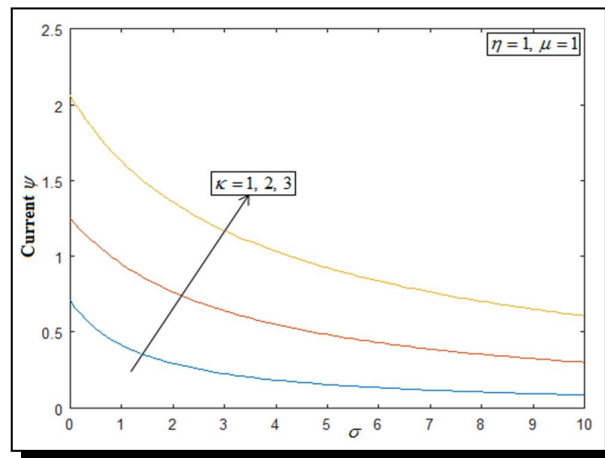
Figure 2



(a) Effect of saturation parameter μ in non-dimensional current ψ

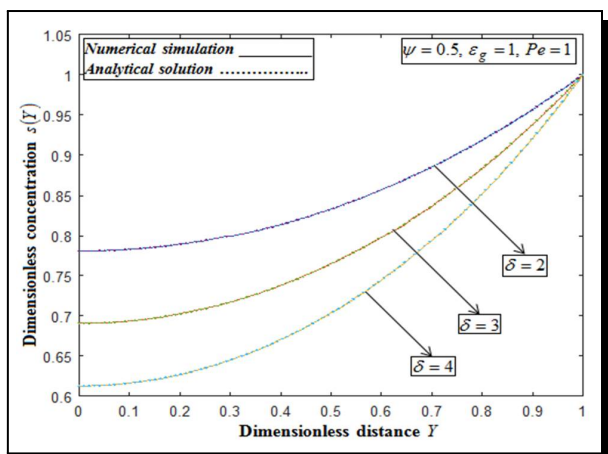


(b) Impact of relative amount of the depletion η in non-dimensional current ψ

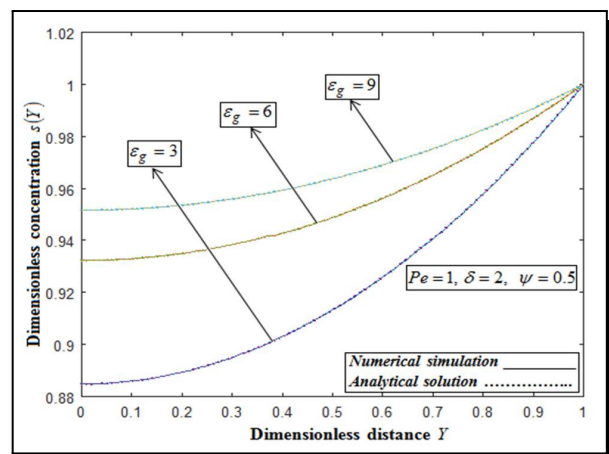


(c) Variation of ratio of enzymatic reaction k in non-dimensional current ψ

Figure 3



(a) Influence of non-dimensional area of the toray carbon paper δ in non-dimensional concentration $s(y)$



(b) Effect of porosity of the film-loaded toray carbon paper ϵ_g in non-dimensional concentration $s(y)$

(Figure continued)

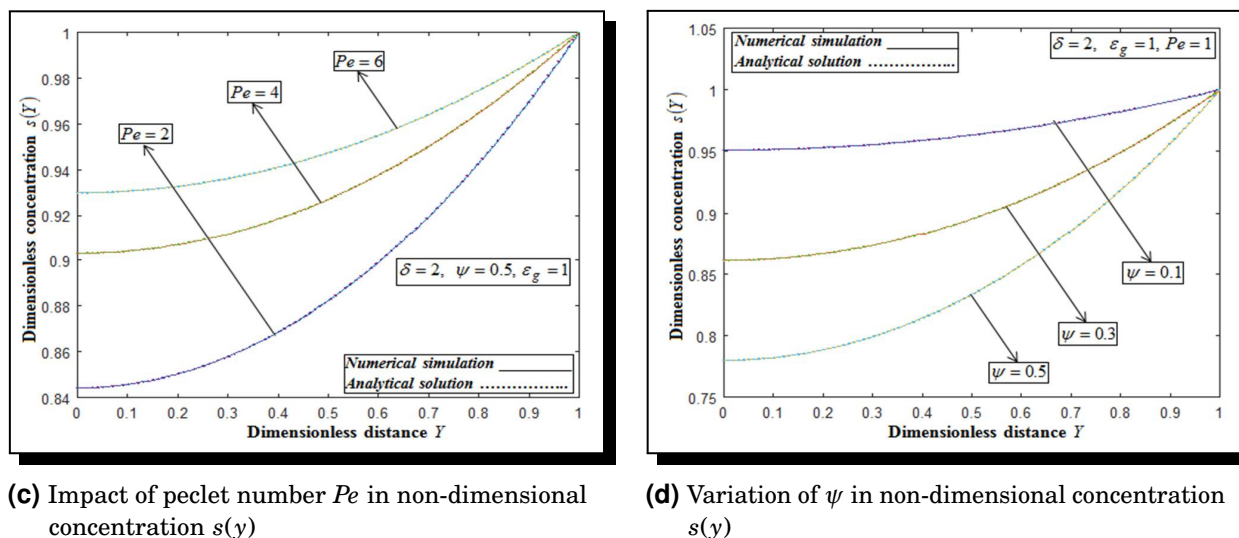


Figure 4

Non-dimensional concentration of substrate. Figure 2 depicts that non-dimensional concentration of substrate S versus the non-dimensional distance X . Figure 2(a) depicts that the value of ratio of enzymatic reaction k get rises, than the non-dimensional concentration get drops. Figures 2(b)-2(d) shows that, by increasing the values of saturation parameter σ , μ and η , than the non-dimensional concentration also get increases.

Non-dimensional current. Figure 3(a) interline that non-dimensional current ψ versus saturation parameter η . From this figure, we noted that the amount of saturation parameter μ increases than the corresponding current get drops. Figure 3(b) displays that the nondimensional current ψ versus the saturation parameter μ . It shows that the values of saturation parameter get raises then the corresponding current get falls. Figure 3(b) interline that the nondimensional current ψ versus the saturation parameter σ . From this figure, it indicates that the quantities of ratio of enzymatic reaction k get rises so does the current.

Non-dimensional concentration of substrate inside porous electrode. Figure 4 demonstrates that the non-dimensional substrate concentration $s(y)$ inside the porous electrode. Figures 4(a) and 4(d) interline that when the values of toray carbon paper δ and ψ increase, the corresponding get drops. Figures 4(b) and 4(c) depicts that by raising the values of porosity of the film-loaded toray carbon paper ε_g and peclot number Pe , so does the concentration.

6. Conclusion

A multiscale porous biocatalytic electrode was investigated mathematically and reported. The semi-analytical expression of the oxidized mediator concentrations, substrate as well as current density was attained. The systems of non-linear equations were resolved employing new homotopy perturbation technique. The approximate analytical solutions that were derived satisfy the numerical simulation very well. This paper also examines how several parameters like rate constants, diffusion coefficient and thickness, voltage, influence the current. The porous electrode model's approximate analytical expressions of the substrate and current were also provided. By employing this method, we can able to resolve the non-linear problems like

Michaelis-Menten kinetics, Non-Michaelis Menten kinetics.

The following results are attained from the above:

- By raising the amount of saturation parameter μ and relative amount of the depletion η , then the corresponding current get drops.
- By raising the amount of ratio of enzymatic reaction k so does the corresponding current.

Appendix A: Approximate Analytical Expression for Equations (2.9)-(2.12) by Employing New Homotopy Perturbation Technique

We attained the approximate analytical solutions to equations (2.9) to (2.12) in this appendix utilizing the new homotopy perturbation approach.

We generate the homotopy shown below for equations (2.9)-(2.12):

$$(1-p) \left[\frac{d^2 M}{dX^2} - \frac{\kappa^2 SM}{\sigma M + \mu S + SM} \right] + p \left[\frac{d^2 M}{dX^2} - \frac{\kappa^2 SM}{\sigma M + \mu S + SM} \right] = 0, \quad (\text{A.1})$$

$$(1-p) \left[\frac{d^2 S}{dX^2} - \frac{\kappa^2 SM}{\eta(\sigma M + \mu S + SM)} \right] + p \left[\frac{d^2 S}{dX^2} - \frac{\kappa^2 SM}{\eta(\sigma M + \mu S + SM)} \right] = 0, \quad (\text{A.2})$$

$$(1-p) \left[\frac{d^2 M}{dX^2} - \frac{\kappa^2 S(1)M}{\sigma M(1) + \mu S(1) + S(1)M(1)} \right] + p \left[\frac{d^2 M}{dX^2} - \frac{\kappa^2 S(1)M}{\sigma M(1) + \mu S(1) + S(1)M(1)} \right] = 0, \quad (\text{A.3})$$

$$(1-p) \left[\frac{d^2 S}{dX^2} - \frac{\kappa^2 SM(1)}{\eta(\sigma M(1) + \mu S(1) + S(1)M(1))} \right] + p \left[\frac{d^2 S}{dX^2} - \frac{\kappa^2 SM(1)}{\eta(\sigma M(1) + \mu S(1) + S(1)M(1))} \right] = 0. \quad (\text{A.4})$$

Equations (A.3) and (A.4) have approximate analytical solutions, which are

$$M = M_0 + pM_1 + p^2M_2 + \dots, \quad (\text{A.5})$$

$$S = S_0 + pS_1 + p^2S_2 + \dots. \quad (\text{A.6})$$

Equating the coefficients of p^0 , after substituting equations (A.5) and (A.6) in equations (A.3) and (A.4), then we attain

$$p^0: \frac{d^2 M_0}{dX^2} - \frac{\kappa^2 M_0}{\sigma + \mu + 1} = 0, \quad (\text{A.7})$$

$$p^0: \frac{d^2 S_0}{dX^2} - \frac{\kappa^2 S_0}{\eta(\sigma + \mu + 1)} = 0. \quad (\text{A.8})$$

Now equations (A.7) and (A.8) becomes

$$\frac{d^2 M_0}{dX^2} - \gamma M_0 = 0, \quad (\text{A.9})$$

$$\frac{d^2 S_0}{dX^2} - \lambda S_0 = 0, \quad (\text{A.10})$$

where

$$\gamma = \frac{\kappa^2}{\sigma + \mu + 1}, \quad (\text{A.11})$$

$$\lambda = \frac{\kappa^2}{\eta(\sigma + \mu + 1)}. \quad (\text{A.12})$$

The boundary conditions for the aforementioned equation are listed below

$$X = 0, M_0 = \frac{1}{(1 + e^{-\epsilon})} = M_\epsilon, \frac{dS_0}{dX} = 0, M_i = 0, \frac{dS_i}{dX} = 0, \quad i = 1, 2, 3, \dots, \tag{A.13}$$

$$X = 1, \frac{dM_0}{dX} = 0, S_0 = 1, \frac{dM_i}{dX} = 0, S_i = 0, \quad i = 1, 2, 3, \dots \tag{A.14}$$

Now solving equations (A.9) and (A.10) by using the equations (A.13) and (A.14), we attained

$$M(x) = M_\epsilon \frac{\cosh \sqrt{\gamma}(X - 1)}{\cosh \sqrt{\gamma}}, \tag{A.15}$$

$$S(x) = \frac{\cosh \sqrt{\lambda}X}{\cosh \sqrt{\lambda}}, \tag{A.16}$$

where γ and λ defined in equations (A.11) and (A.12).

Appendix B: Approximate Analytical Expression for Equation (2.18) by Employing Ananthaswamy-Sivasankari Method

The semi-analytical expression for the non-dimensional substrate concentration inside the porous electrode $s(y)$ is attained approximately by utilizing ASM is described below.

In order to satisfy the boundary condition, the approximate analytical solution to equation (2.18) is as follows:

$$s(Y) = Ae^{aY} + Be^{-aY}, \tag{B.1}$$

$$\frac{ds}{dY} = aAe^{aY} - aBe^{-aY}. \tag{B.2}$$

Employing the boundary conditions in equations (2.19) and (2.20), we attained the value of the parameters A and B as:

$$A = B, \quad A = \frac{1}{e^a + e^{-a}}. \tag{B.3}$$

Thus, equation (B.1), becomes

$$s(Y) = \frac{e^{aY} + e^{-aY}}{e^a + e^{-a}}. \tag{B.4}$$

Now by utilizing equation (B.4) in equation (2.20) and on simplification, we yield

$$a^2 \left(\frac{e^{aY} + e^{-aY}}{e^a + e^{-a}} \right) + \frac{Pe}{\epsilon_g} a \left(\frac{e^{aY} - e^{-aY}}{e^a + e^{-a}} \right) - \frac{\delta\psi}{\epsilon_g} = 0. \tag{B.5}$$

Now taking, equation (B.5) becomes

$$a^2 + \frac{Pe}{\epsilon_g} a \tanh h(a) - \frac{\delta\psi}{\epsilon_g} = 0. \tag{B.6}$$

On solving equation (B.6) by substituting the values of $\delta = 7$, $\psi = 0.5$, $\epsilon_g = 1$, $Pe = 1$, we get the value of the parameter m as follows:

$$a = -1.4741. \tag{B.7}$$

Hence an semi-analytical expressions of the non-dimensional substrate concentration inside the porous electrode $s(y)$ equation (2.18) is obtained as

$$s(Y) = \frac{e^{aY} + e^{-aY}}{e^a + e^{-a}}. \tag{B.8}$$

Appendix C: Nomenclature

| <i>Symbols</i> | <i>Meanings</i> |
|-----------------|--|
| δ | Dimensionless area of the Toray carbon paper |
| η | Relative amount of depletion of the substrate and oxidized mediator within the film |
| μ, σ | Saturation parameter for mediator and substrate |
| v | Velocity of fluid element, $\text{cm}^2 \text{s}^{-1}$ |
| ψ | Dimensionless current |
| ψ_P | Dimensionless current for porous electrode model |
| Pe | Peclet number |
| ε | Dimensionless potential |
| ε_g | Porosity of the film-loaded Toray carbon paper |
| a | Surface area per unit volume of the Toray carbon paper, $\text{cm}^3 \text{cm}^{-3}$ |
| D_M | Diffusion coefficient for mediator, $\text{cm}^2 \text{s}^{-1}$ |
| D_S | Diffusion coefficient for substrate, $\text{cm}^2 \text{s}^{-1}$ |
| E | Concentration of enzyme, mol, cm^{-3} |
| E_0 | Formal potential of the mediator couple, V (SHE) |
| F | Faraday constant, $As \text{mol}^{-1}$ |
| I | Current density, A |
| j | Flux, $\text{cm}^2 \text{s}^{-1}$ |
| k | Ratio of the enzymatic reaction within in the film to the diffusion of the oxidized mediator |
| k_{cat} | Electron turnover number, s^{-1} |
| K_M, K_S | Michaelis-Menten rate constant for the mediator and substrate, mol, cm^{-3} |
| L | Thickness of the Toray carbon paper, μm |
| m | Dimensionless concentration of oxidized mediator |
| M_{ox} | Concentration of oxidized mediator, mol, cm^{-3} |
| M_0 | Reference concentration for mediator, mol, cm^{-3} |
| N | Number of electrons <i>Nil</i> |
| R | Universal gas constant, $J \text{mol}^{-1} \text{K}^{-1}$ |
| s | Dimensionless concentration of substrate |
| S | Concentration of substrate, mol, cm^{-3} |
| S_0 | Reference concentration for mediator, mol, cm^{-3} |
| T | Absolute temperature, K |
| x | Dimensional position within the hydrogel film, cm |
| X | Dimensionless distance from the film interface |
| y | Dimensional position within the Porous electrode, μm |
| Y | Dimensionless Position within the porous electrode |

Competing Interests

The authors declare that they have no competing interests.

Authors' Contributions

All the authors contributed significantly in writing this article. The authors read and approved the final manuscript.

References

- [1] G. Adomian, *Solving Frontier Problems of Physics: The Decomposition Method*, 1st edition, Springer, Dordrecht, xiv + 354 pages (1993).
- [2] V. Ananthaswamy and S. Narmatha, Semi-analytical solution for surface coverage model in an electrochemical arsenic sensor using a new approach to homotopy perturbation method, *International Journal of Modern Mathematical Sciences* **17**(2) (2019), 85 – 110.
- [3] V. Ananthaswamy, R. Shanthakumari and M. Subha, Simple analytical expressions of the non-linear reaction diffusion process in an immobilized biocatalyst particle using the new homotopy perturbation method, *Review of Bioinformatics and Biometrics* **3** (2014), 22 – 28.
- [4] O. E. Barcia, E. D'Elia, I. Frateur, O. R. Mattos, N. Pébère and B. Tribollet, Application of the impedance model of de Levie for the characterization of porous electrodes, *Electrochimica Acta* **47**(13-14) (2002), 2109 – 2116, DOI: 10.1016/S0013-4686(02)00081-6.
- [5] E. O. Barnes, X. Chen, P. Li and R. G. Compton, Voltammetry at porous electrodes: A theoretical study, *Journal of Electroanalytical Chemistry* **720-721** (2014), 92 – 100, DOI: 10.1016/j.jelechem.2014.03.028.
- [6] P. N. Bartlett and K. F. E. Pratt, Theoretical treatment of diffusion and kinetics in amperometric immobilized enzyme electrodes Part I: Redox mediator entrapped within the film, *Journal of Electroanalytical Chemistry* **397**(1-2) (1995), 61 – 78, DOI: 10.1016/0022-0728(95)04236-7.
- [7] D.-S. Chan, D.-J. Dai and H.-S. Wu, Dynamic modeling of anode function in enzyme-based biofuel cells using high mediator concentration, *Energies* **5**(7) (2012), 2524 – 2544, DOI: 10.3390/en5072524.
- [8] S. Cosnier, A. J. Gross, A. Le Goff and M. Holzinger, Recent advances on enzymatic glucose/oxygen and hydrogen/oxygen biofuel cells: Achievements and limitations, *Journal of Power Sources* **325** (2016), 252 – 263, DOI: 10.1016/j.jpowsour.2016.05.133.
- [9] T. Q. N. Do, M. Varničić, R. Hanke-Rauschenbach, T. Vidaković-Koch and K. Sundmacher, Mathematical modeling of a porous enzymatic electrode with direct electron transfer mechanism, *Electrochimica Acta* **137** (2014), 616 – 626, DOI: 10.1016/j.electacta.2014.06.031.
- [10] J. Galceran, S. L. Taylor and P. N. Bartlett, Modelling the steady-state current at the inlaid disc microelectrode for homogeneous mediated enzyme catalysed reactions, *Journal of Electroanalytical Chemistry* **506**(2) (2001), 65 – 81, DOI: 10.1016/S0022-0728(01)00503-4.
- [11] J.-H. He, A coupling method of a homotopy technique and a perturbation technique for non-linear problems, *International Journal of Non-Linear Mechanics* **35**(1) (2000), 37 – 43, DOI: 10.1016/S0020-7462(98)00085-7.
- [12] J.-H. He, A simple perturbation approach to Blasius equation, *Applied Mathematics and Computation* **140**(2-3) (2003), 217 – 222, DOI: 10.1016/S0096-3003(02)00189-3.
- [13] J.-H. He, Homotopy perturbation method: A new nonlinear analytical technique, *Applied Mathematics and Computation* **135**(1) (2003), 73 – 79, DOI: 10.1016/S0096-3003(01)00312-5.

- [14] J.-H. He, Homotopy perturbation technique, *Computer Methods in Applied Mechanics and Engineering* **178**(3-4) (1999), 257 – 262, DOI: 10.1016/S0045-7825(99)00018-3.
- [15] J. H. He, Some asymptotic methods for strongly nonlinear equations, *International Journal of Modern Physics B* **20**(10) (2006), 1141 – 1199, DOI: 10.1142/S0217979206033796.
- [16] X. Ke, J. M. Prael, J. I. D. Alexander and R. F. Savinell, Redox flow batteries with serpentine flow fields: Distributions of electrolyte flow reactant penetration into the porous carbon electrodes and effects on performance, *Journal of Power Sources* **384** (2018), 295 – 302, DOI: 10.1016/j.jpowsour.2018.03.001.
- [17] D. Leech, P. Kavanagh and W. Schuhmann, Enzymatic fuel cells: Recent progress, *Electrochimica Acta* **84** (2012) 223 – 234, DOI: 10.1016/j.electacta.2012.02.087.
- [18] A. Meena and L. Rajendran, Analysis of a pH-based potentiometric biosensor using the Homotopy perturbation method, *Chemical Engineering & Technology* **33**(12) (2010), 1999 – 2007, DOI: 10.1002/ceat.200900580.
- [19] N. Mehala and L. Rajendran, Analysis of mathematical modelling on potentiometric biosensors, *International Scholarly Research Notices* **2014**(1) (2014), 582675, DOI: 10.1155/2014/582675.
- [20] M. M. Mousa and S. F. Ragab, Applications of the homotopy perturbation method to linear and non-linear Schrödinger equations, *Zeitschrift für Naturforschung A* **63**(3-4) (2008), 140 – 144, DOI: 10.1515/zna-2008-3-404.
- [21] B. Nam and R. T. Bonnecaze, Analytic models of the infinite porous rotating disk electrode, *Journal of the Electrochemical Society* **154**(10) (2007), F191, DOI: 10.1149/1.2759834.
- [22] M. Rasi, K. Indira and L. Rajendran, Approximate analytical expressions for the steady-state concentration of substrate and cosubstrate over amperometric biosensors for different enzyme kinetics, *International Journal of Chemical Kinetics* **45**(5) (2013), 322 – 336, DOI: 10.1002/kin.20768.
- [23] V. Vijayalakshmi, V. Ananthaswamy and J. A. Jothi, Semi-analytical study on non-isothermal steady R-D equation in a spherical catalyst and biocatalyst, *CFD Letters* **15**(12) (2023), 60 – 76, DOI: 10.37934/cfdl.15.12.6076.
- [24] A.-M. Wazwaz, The variational iteration method for solving linear and nonlinear ODEs and scientific models with variable coefficients, *Open Engineering* **4**(1) (2014), 64 – 71, DOI: 10.2478/s13531-013-0141-6.
- [25] H. Wen, K. Ramanujam and S. C. Barton, Multiscale carbon materials as supports for bioelectrodes, *ECS Transactions* **13**(21) (2008), 67, DOI: 10.1149/1.3036212.

